Haynes, Matthew A.; Lohmann, Birgit
Comparative study of argon 3p electron-impact ionization at low energies Physical Review A, 2001; 64:004701-1-004701-4

http://link.aps.org/doi/10.1103/PhysRevA.64.044701

Comparative study of argon 3*p* electron-impact ionization at low energies

Matthew A. Haynes and Birgit Lohmann*
School of Science, Griffith University, Nathan, Queensland 4111, Australia
(Received 26 January 2001; published 6 September 2001)

An experimental and theoretical study of electron-impact ionization of the 3*p* orbital in argon is presented. The (*e*,2*e*) technique was used to measure the relative triple-differential cross section for this process in the coplanar asymmetric geometry. The experimental results were obtained at an incident electron energy of 113.5 eV, a scattering angle of 15°, and ejected electron energies of 10, 7.5, 5, and 2 eV. The experimental data are compared with a distorted-wave Born approximation (DWBA) calculation, and also with previous results for argon 3*s* ionization obtained under identical kinematic conditions. Discrepancies between the experimental and theoretical data are attributed to the effects of charge-cloud polarization and higher-order scattering processes, which are not incorporated in the DWBA calculation.

DOI: 10.1103/PhysRevA.64.044701 PACS number(s): 34.80.Dp

Electron-impact ionization is one of the most fundamental collision processes in atomic physics. However, as highlighted recently by Rescigno *et al.* [1], even the simplest case of electron-impact ionization of atomic hydrogen has posed an almost intractable theoretical problem. Nevertheless, recent progress in the numerical solution of the Schrödinger equation for the problem of three charged particles in the final state suggests that electron-hydrogen ionization is close to solution [1–3].

Experimentally, the methods used to study electron-impact ionization are now sophisticated enough to explore ionization from a range of atomic and molecular targets, and to investigate processes involving inner-shell or excited-state ionization, and ionization processes proceeding via resonant states. The challenge now to theory is to extend the new ''exact'' methods to many-electron atoms and molecules, although as noted by Rescigno *et al.* numerous other theoretical methods are used to study ionization, and some of them give ''surprisingly good'' [1] results. Importantly, some of these other approaches allow the treatment of electron-impact ionization of more complicated atoms.

In this Brief Report we present experimental data for electron-impact ionization of the 3*p* orbital in argon. This is a complementary study, under identical kinematic conditions, to our previous work on low-energy electron-impact ionization of the 3*s* inner valence orbital in argon [4]. The experiments yield a relative measure of the triple-differential cross section (TDCS). The TDCS contains the most detailed information about the ionization process, as it gives the ionization probability for producing electrons with specific energies and emission angles. In our earlier study of argon 3*s* ionization, our experimental results were compared with calculations performed in the distorted-wave Born approximation (DWBA). The DWBA is a theoretical approach that has been successfully employed to model electron-impact ionization across a range of targets and kinematics, particularly at higher energies (see, for example, Refs. [5–7]). However, large discrepancies were found between our experimental argon 3*s* results and DWBA calculations. One problem with the DWBA is that Coulombic repulsion between the two outgoing electrons in the final state (postcollision interaction, or PCI) and target charge-cloud polarization are not treated by the model, although a number of attempts have been made to include these effects as ''add-ons'' [8]. In Ref. [8], a calculation of this type was compared with measurements of the TDCS for argon 3*p* ionization in coplanar symmetric kinematics (in the latter, the outgoing electrons have equal energies and angles, unlike the present experiments, the geometry of which will be discussed in more detail below). Even with the inclusion of PCI and polarization, the agreement with experiment was very poor at low energies. These effects are likely to become more important as the energy of the electrons decreases, and hence the correctness of their treatment also becomes more important. Measurements of the TDCS for ionization of different orbitals in the same target, but with the same kinematics, may assist in ascertaining which (if any) of these effects is the origin of the discrepancies between theory and experiment.

The experimental geometry used in the experiments described here is illustrated in Fig. 1. The incident electron, scattered electron, and ejected electron are detected in a single plane (the scattering plane, defined by the incident and scattered electron momentum vectors). In the outgoing channel, the scattered electron is defined to be that with the higher energy. The kinematical arrangement used is termed the coplanar asymmetric geometry, in which the scattered electron is detected at a fixed forward angle θ_a, in coinci-

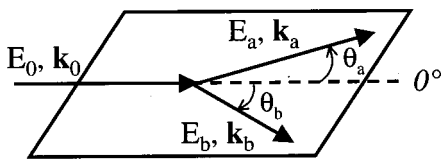

FIG. 1. Diagram of the coplanar asymmetric kinematics employed in the present measurements. The incident electron has energy and momentum E_0, $\mathbf{k}_0$. The scattered electron is detected at a scattering angle θ_a with energy E_a, while the ejected electron is detected with energy E_b at varying angles θ_b. θ_a and θ_b are measured from 0°, as shown.

*Author to whom correspondence should be addressed. Electronic address: B.Lohmann@sct.gu.edu.au

dence with an ejected electron detected at varying angles θ_b. The energy of the scattered electron is chosen to be much higher than that of the ejected electron, and is related to the energy of the incident electron by energy conservation:

$$E_0 = E_a + E_b + \varepsilon_i ,$$

where E_0 is the incident electron energy, E_a and E_b are the scattered and ejected electron energies, respectively, and ε_i is the binding energy of an electron in the orbital that is being ionized. The experimental conditions for these measurements were $E_0 = 113.5$ eV, $\theta_a = 15°$, and $E_b = 10$, 7.5, 5, or 2 eV. The binding energy of the $3p$ orbital was taken to be 15.8 eV.

The apparatus comprises an electron gun delivering an incident electron beam with a current of approximately 2 μA which crosses a target gas beam at right angles. Electrons emitted from the ionization process are detected by channeltrons positioned at the exits of two identical hemispherical electron energy analyzers, which are equipped with electron optical lenses on the input. The scattering plane is constrained to be perpendicular to the atomic gas beam. Fast-timing electronics are used to determine whether two detected electrons have originated from the same ionization event. Further experimental details may be found in Ref. [4]. Note that the experimental cross-section data presented here are on a relative scale. In order to measure absolute cross sections it is necessary to know accurately quantities such as the gas number density in the interaction region and the absolute transmission efficiencies of the two electron energy analyzers, which are very problematic to determine in coincidence experiments.

The distorted-wave Born approximation calculations presented here have been performed using a DWBA code provided by McCarthy [9]. The form of the approximation to the TDCS in this formulation is

$$\frac{d^5\sigma}{d\Omega_a d\Omega_b dE_a} = (2\pi)^4 \frac{k_a k_b}{k_0} \times \sum_{\text{av}} |\langle \chi^{(-)}(\mathbf{k}_a)\chi^{(-)}(\mathbf{k}_b)|v_3|\alpha\chi^{(+)}(\mathbf{k}_0)\rangle|^2 .$$

Here Ω_a and Ω_b are the solid angles of detection of electrons a and b (scattered and ejected electrons) while $\mathbf{k}_0$, $\mathbf{k}_a$, and $\mathbf{k}_b$ are the linear momenta of the incident and outgoing electrons. $\chi^{(+)}(\mathbf{k}_0)$ is a distorted wave representing the incident electron while $\chi^{(-)}(\mathbf{k}_a)$ and $\chi^{(-)}(\mathbf{k}_b)$ are distorted waves representing the fast outgoing scattered electron and slow outgoing ejected electron, respectively. α is a Hartree-Fock representation of the target orbital and v_3 is the electron-electron interaction. In the calculations presented here, the incident electron distorted wave is calculated in a distorting potential that is generated using Hartree-Fock wave functions to represent the neutral target atom. The ejected electron distorted wave is calculated in a potential produced using a Hartree-Fock representation of the ion. The scattered electron distorted wave was calculated either in the atom potential or in the same ion potential used for the

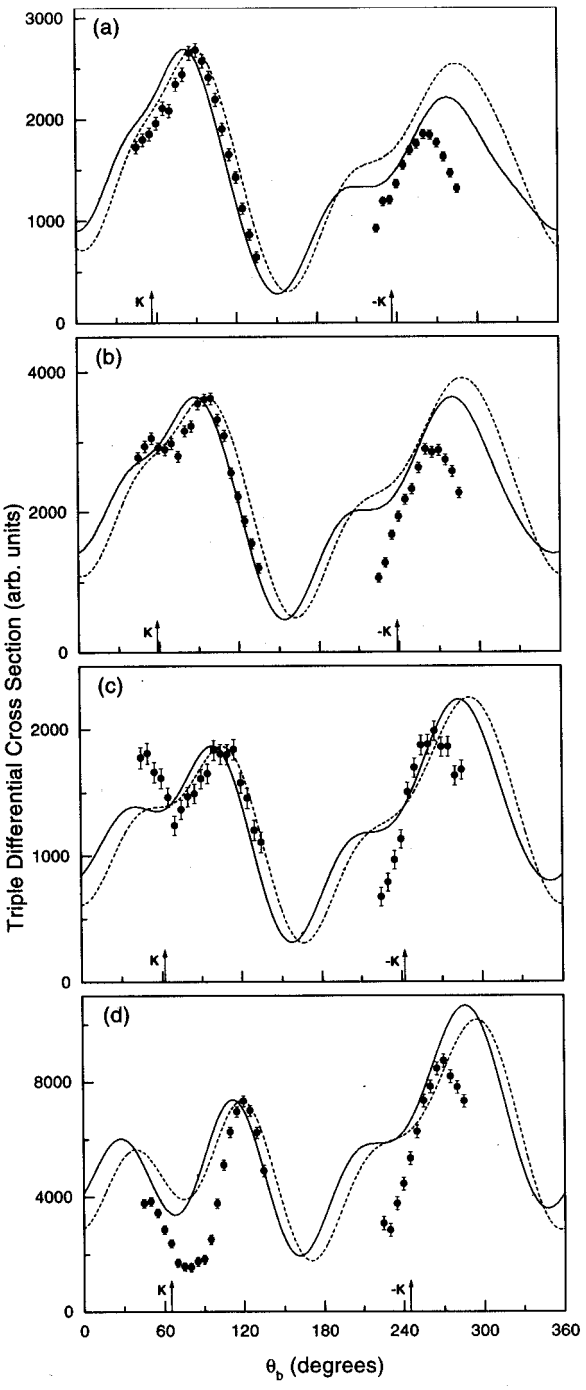

FIG. 2. Experimental and theoretical TDCS's for ionization of the $3p$ orbital in argon. In each case the solid points are the experimental data, the solid line is a DWBA calculation using the atom potential for the scattered electron distorted wave, and the dashed line is a DWBA calculation employing the ion potential for the scattered electron distorted wave. The momentum transfer direction $\mathbf{K}$ and $-\mathbf{K}$ are indicated on each plot. The experimental conditions were $E_0 = 113.5$ eV, $\theta_a = 15°$, and $E_b =$ (a) 10, (b) 7.5, (c) 5, (d) 2 eV.

ejected electron distorted wave. Exchange is included by using the Furness-McCarthy [10] equivalent local exchange potential in the spin-averaged static-exchange potential used as the distorting potential.

The results are shown in Figs. 2(a)–2(d). The theoretical curves are the solid and dashed lines, with the former corresponding to the case where the scattered electron distorted wave has been calculated in the atom potential, and the latter corresponding to the case where it has been calculated in the ion potential. The experimental data have been normalized to the calculations in the region of the peak near 100°. In Fig. 2(a), which corresponds to a slow electron energy of 10 eV, two main structures are apparent in the cross section. The peak at forward angles is referred to as the binary peak, and is the result of an impulsive collision between the incident electron and the target electron. The peak at backward angles is referred to as the recoil peak, and is attributed to a double scattering process in which the ejected electron undergoes an elastic backscattering from the residual ion core, before being emitted from the atom. Also shown on the plot is the direction of the momentum transfer vector $\mathbf{K}=\mathbf{k}_0-\mathbf{k}_a$, which is an axis of symmetry for the TDCS in first-order theories such as the Born approximation. It is apparent that the calculations are in good agreement in terms of shape with the experimental data in the region of the binary peak; this contrasts with what was observed for argon $3s$ ionization [4], where there was a large shift ($\sim$20°) between the experimental and theoretical positions of this peak. In the recoil region the calculations overestimate the size of the recoil peak and put the peak at too large an angle; a similar effect was observed for argon $3s$ ionization. Note that the calculations predict structure in both the binary and recoil peaks, which also appears to be present in the experimental data, certainly in the binary region. This structure is related to the form of the momentum-space distribution for a p orbital [11]. As the ejected electron energy decreases [Figs. 2(b)–2(d)], we see that agreement between theory and experiment in the binary region is good at 7.5 eV, and worsens somewhat in going to 5 and 2 eV ejected electron energy. The major discrepancy is in the description of the double-peaked structure in the binary region, particularly the depth of the ''dip.'' The position of the binary structure is still well described, however, which is in complete contradistinction to the case for argon $3s$ ionization, where at each of the above ejected electron energies there were large differences between the theoretical and experimental positions of the binary peak.

For each ejected electron energy, the calculations overestimate the relative size of the recoil peak, and also predict its position incorrectly. Comparison with our previous argon $3s$ results is more difficult for the case of the recoil peak, since the position of the recoil structure for the $3s$ orbital case was such that, combined with apparatus constraints, it was only possible to measure part of the recoil peak. Major discrepancies were observed between the DWBA calculations and the experimental data, but it was not possible to determine if these were a result of an incorrect angular position or an incorrect magnitude (or both).

As the distorted-wave Born approximation does not include PCI between the two outgoing electrons, one may surmise that differences between theory and experiment in the angular positions of the peaks may be the result of Coulomb repulsion in the final channel. However, although the scattered electron energy in our previous measurements on argon $3s$ ionization was somewhat lower than that in the present $3p$ measurements due to the different binding energies of the orbitals (29.3 versus 15.8 eV), it is unlikely that this would result in substantially different PCI effects in the two cases, given that E_a is still much larger than E_b. Hence the fact that there is no shift of the binary peak in the $3p$ case relative to the theoretical calculations indicates that the discrepancy observed in the $3s$ measurements must be attributed to another effect. Keeping the incident energy the same in the two sets of measurements should rule out target polarization in the incoming channel as the culprit; however, the polarizability of the ion after the process will be quite different for the case where there is a $3s$ hole surrounded by a closed $3p$ shell compared with the case of a hole in the outer valence shell.

The discrepancies between theory and experiment in the recoil region appear to be present for both the $3p$ and $3s$ ionization, which suggests that the recoil scattering is being treated incorrectly; the differences may be a signature of higher-order scattering processes that are not considered in the DWBA.

Some general remarks can be made about the level of agreement between theory and experiment in Fig. 2. In each case the theoretical calculation using the ion potential appears to be in somewhat better agreement with the experimental data in the region of the binary peak. This may appear to be somewhat surprising as the scattered electron experiences an ion core shielded by the relatively slow ejected electron—hence one might expect the atom potential to give better agreement. However, as has been pointed out by Whelan *et al.* [12], it appears to be largely fortuitous which of the two approximations gives better agreement in any particular case. Clearly, neither calculation is able to reproduce the evolution of the structure in the binary peak as the ejected electron energy is reduced. In going from 10 to 2 eV ejected electron energy, the magnitude of the momentum transfer varies only slightly (0.79 to 0.76 a.u.), yet there are dramatic variations in the shape of the binary peak. The theory reproduces the trend of these variations, but not the detail.

At present, the DWBA appears to be one of the few theoretical approximations that can be relatively easily applied to the problem of electron-impact ionization of rare-gas atoms. However, the results presented here indicate that additional effects must be incorporated into the DWBA, such as polarization of the residual ion in the outgoing channel, if it is to be successful in describing such processes at low incident energies. Higher-order effects in electron-impact ionization have recently been very successfully treated in the second-Born calculations of Marchalant *et al.* [13] on excitation ionization in helium, and it would be of considerable interest to see the application of that approach to the present results.

This work was supported by a grant from the Australian Research Council.

[1] T. N. Rescigno *et al.*, Science **286**, 2474 (1999).
[2] I. Bray, J. Phys. B **33**, 581 (2000).
[3] A. T. Stelbovics, Phys. Rev. Lett. **84**, 1878 (2000).
[4] M. A. Haynes and B. Lohmann, J. Phys. B **33**, 4711 (2000).
[5] S. J. Cavanagh and B. Lohmann, J. Phys. B **30**, L231 (1997).
[6] S. J. Cavanagh and B. Lohmann, Phys. Rev. A **57**, 2718 (1998).
[7] S. J. Cavanagh *et al.*, Phys. Rev. A **60**, 2977 (1999).
[8] S. Rioual *et al.*, J. Phys. B **30**, L475 (1997).
[9] I. E. McCarthy, Aust. J. Phys. **48**, 1 (1995).
[10] J. B. Furness and I. E. McCarthy, J. Phys. B **6**, 2280 (1973).
[11] A. Lahmam-Bennani *et al.*, J. Phys. B **16**, 121 (1983).
[12] C. T. Whelan *et al.*, in *(e,2e) and Related Processes*, edited by C. T. Whelan, H. R. J. Walters, A. Lahmam-Bennani, and H. Ehrhardt (Kluwer, London, 1993), p. 1.
[13] P. J. Marchalant *et al.*, J. Phys. B **33**, L749 (2000).